Signal Design for Ultra-wideband Radio *

Robert A. Scholtz, P. Vijay Kumar, and Carlos J. Corrada-Bravo

Department of Electrical Engineering
University of Southern California, Los Angeles, CA 90089-2565

Abstract. Research in the design of ultra-wideband (UWB) radio systems suggests different kinds of signal design criteria. After an introduction to UWB radio, a variety of sequence design problems, motivated by UWB system constraints, will be presented. Design for time-hopping, for spectral flatness, for rapid acquisition, and for multiple access will be discussed, and some sample designs will be presented.

1 Introduction to UWB Radio

When the 3 dB bandwidth of a radio signal becomes 25% or more of the signal's center frequency, most agree that this radio should be called *ultra-wideband* (UWB). The combination of a relatively large bandwidth at a relatively low center frequency provides two kinds of dividends. First, of all radios at the same center frequency, an ultra-wideband radio should provide the finest time resolution in a well-designed receiver, and hence have potential advantages in ranging and multipath mitigation. Second, of all radios with the same bandwidth, ultra-wideband radios operate in the lowest frequency bands and hence have the best chance to propagate through most materials.

One major problem that UWB radios must solve is the satisfactory coexistence of UWB radio signals with the myriad of other narrowband and wideband signals with which they must simultaneously share their frequency bands [1]. This implies that UWB radios should employ spread-spectrum methods to protect them against the interference that they will inevitably encounter from other radio systems. It also implies that UWB radios can only radiate small amounts of power in each of the narrow frequency bands of other radio systems to avoid interfering with them. This latter issue is a matter for the appropriate regulatory entity to oversee.

Regulation of UWB radio currently is being considered in the United States, and may take the form of an upper bound on the radiated power spectral density of the UWB system. Then, the efficiency and performance of the UWB system will depend to a great extent on the flatness and range of its radiated power spectral density.

The technology used to implement UWB radio depends on the frequency band in which the radio must operate. Modulations in UWB radios usually

* This work was supported in part by the Office of Naval Research under grant N00014-96-1-1192 (subcontract from the University of Puerto Rico), and by the National Science Foundation under grant ANI-9730556.

are constructed from trains of very short pulses whose width often is in the range of a few nanoseconds to fractions of a nanosecond, giving bandwidths on the order of gigahertz. Since the ability of an antenna to radiate efficiently decreases as frequency approaches zero, the pulse shapes are generally chosen to have little or no energy content as frequency approaches zero. Hence pulses tend to have balanced positive and negative excursions, e.g., one period of a sinusoid, or the derivative of a Gaussian pulse.

Modulation formats vary, but UWB radios generally transmit several pulses per data bit and use coherent detection of the pulse train. The radios usually produce carrierless signals and do not use mixers for the purpose of changing the frequency band of a signal. Some systems resemble baseband direct-sequence spread-spectrum systems and others resemble baseband time-hopped spread-spectrum signals [2]. Digital modulation of these kinds of signals is accomplished by added time shifting or polarity reversal.

We will now describe several signal-design problems motivated by this description of UWB radio.

2 Time-Hopping Signal Models

Time hopping for spectral spreading may provide implementation advantages and may be desirable in ranging systems because it may be easier to find the leading edge of an isolated received pulse signal. One possible form of an unmodulated time-hopping ultra-wideband signal generator is shown in Figure 1. In this example, before data modulation, the i^{th} time-hopped signal is of the form

$$s^{(i)}(t) = \sum_j p(t - jT_{\text{f}} - c_j^{(i)} T_{\text{c}}) = \sum_n a_n^{(i)} p(t - nT_{\text{c}})\,, \tag{1}$$

where we assume for simplicity that one frame time T_{f} is composed of N_{f} such slots, i.e., $N_{\text{f}} T_{\text{c}} = T_{\text{f}}$. The integer time-hopping code $\{c_j^{(i)}\}$, $0 \le c_j^{(i)} < N_{\text{f}}$, has period N. Then the quantity $a_n^{(i)}$ is defined as

$$a_n^{(i)} = \begin{cases} 1 & \text{if there is an integer } j \text{ such that } n = jN_{\text{f}} + c_j^{(i)}\,, \\ 0 & \text{otherwise.} \end{cases} \tag{2}$$

A signal then is described totally by which time slots are occupied and which slots are not.

Lets assume for simplicity that the time width T_{w} of a pulse $p(t)$ is less than T_{c}. Then the normalized periodic correlation between the signals of users i and j is

$$\tilde{R}_{ij}(n_\tau T_{\text{c}}) \triangleq \frac{R_{ij}(n_\tau T_{\text{c}})}{R_{ii}(0)} = \frac{1}{N} \underbrace{\sum_{n=0}^{NN_{\text{f}}-1} a_n^{(i)} a_{n \ominus n_\tau}^{(j)}}_{\text{coincidence correlation}}\,. \tag{3}$$

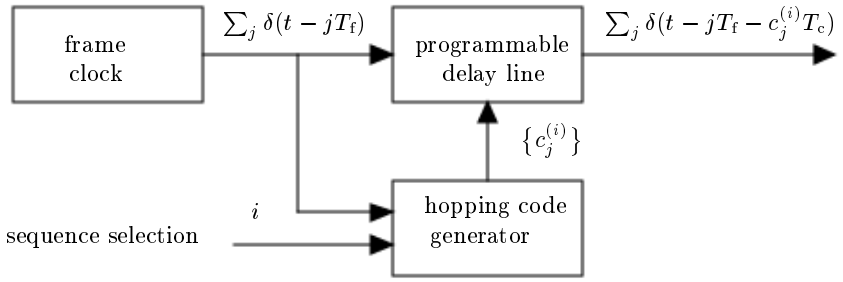

Fig. 1. A framed time-hopping sequence generator.

This equation displays the normalized periodic coincidence correlation between the two transmitted signals when one is shifted by an integer number n_τ of slot widths relative to the other. The quantity N is the period of the time-hopping sequence design measured in frame times, and hence the period of any of the binary sequences $\{a_n^{(i)}\}$ is NN_f, i.e., $a_n^{(i)} = a_{n+NN_f}^{(i)}$ for all n and i. The notation $\ominus$ in (3) denotes subtraction modulo NN_f, leading to the periodic nature of the computation. The peak value 1 occurs when $i = j$ and $n_\tau = 0$.

For the moment let's assume that, except for the peak value, the design objective from an auto-correlation viewpoint is to make the periodic coincidence correlation as small as possible. As structured here, the design requires that one and only one slot in each frame be occupied by a pulse. Hence $a_n^{(i)} = 0$ for all but one value of n in each range $jN_f \le n < (j+1)N_f$ for each value of j. Let's display this graphically in an $N_f \times N$ matrix by mapping the sequence $\{a_n^{(i)}\}$ into the matrix $\mathbf{A}^{(i)}$ as follows.

$$a_0^{(i)}, a_1^{(i)}, \ldots, a_{NN_f-1}^{(i)} \iff \underbrace{\begin{bmatrix} a_0^{(i)} & a_{N_f}^{(i)} & a_{2N_f}^{(i)} & \cdots & a_{(N-1)N_f}^{(i)} \\ a_1^{(i)} & a_{N_f+1}^{(i)} & a_{2N_f+1}^{(i)} & \cdots & a_{(N-1)N_f+1}^{(i)} \\ \vdots & \vdots & \vdots & \ddots & \vdots \\ a_{N_f-1}^{(i)} & a_{2N_f-1}^{(i)} & a_{3N_f-1}^{(i)} & \cdots & a_{NN_f-1}^{(i)} \end{bmatrix}}_{\triangleq \mathbf{A}^{(i)}} \tag{4}$$

That is, one period of the sequence is entered into the matrix $\mathbf{A}^{(i)}$, filling in order the first column, the second column, etc. The constraint of one pulse per frame time translates to exactly one 1 entry and $N_f - 1$ entries which are 0 in each column of the matrix $\mathbf{A}^{(i)}$. So for example, the sequence with period 16 and 4 slots per frame, with slots 0, 7, 9, and 14, occupied by pulses

is represented by the matrix

$$N_{\mathrm{f}} = N = 4 \text{ and } a_0^{(i)} = a_7^{(i)} = a_9^{(i)} = a_{14}^{(i)} = 1 \iff \begin{bmatrix} 1\,0\,0\,0 \\ 0\,0\,1\,0 \\ 0\,0\,0\,1 \\ 0\,1\,0\,0 \end{bmatrix} . \tag{5}$$

This is reminiscent of frequency-hopping designs in which the column index represents time and the row index represents frequency, but in this development both the row and column indices represent time shifts.

The sequence notation is clumsy for matrices, so let's doubly index the elements of the matrix by defining $b_{jk}^{(i)} = a_{kN_{\mathrm{f}}+j}$ where $0 \le j < N_{\mathrm{f}} - 1$ and $0 \le k < N$. Equivalently,

$$\mathbf{A}^{(i)} \triangleq \begin{bmatrix} b_{00}^{(i)} & b_{01}^{(i)} & b_{02}^{(i)} & \cdots & b_{0,N-1}^{(i)} \\ b_{10}^{(i)} & b_{11}^{(i)} & b_{12}^{(i)} & \cdots & b_{1,N-1}^{(i)} \\ \vdots & \vdots & \vdots & \ddots & \vdots \\ b_{N_{\mathrm{f}}-1,0}^{(i)} & b_{N_{\mathrm{f}}-1,1}^{(i)} & b_{N_{\mathrm{f}}-1,2}^{(i)} & \cdots & b_{N_{\mathrm{f}}-1,N-1}^{(i)} \end{bmatrix} \tag{6}$$

Now let's define the inner product of two arbitrary real $N_{\mathrm{f}} \times N$ matrices $\mathbf{A}$ and $\mathbf{B}$ of the same dimensions to be

$$(\mathbf{A}, \mathbf{B}) \triangleq \sum_m \sum_n a_{mn} b_{mn} \tag{7}$$

where the sums cover the full range of indices of the matrices. If we compute the inner product of two of the binary signal matrices, the result is a recognizable correlation, namely

$$\left(\mathbf{A}^{(i)}, \mathbf{A}^{(j)}\right) = \sum_{m=0}^{N_{\mathrm{f}}-1} \sum_{n=0}^{N-1} b_{mn}^{(i)} b_{mn}^{(j)} = \sum_{n=0}^{NN_{\mathrm{f}}-1} a_n^{(i)} a_n^{(j)} = N \cdot \tilde{R}_{ij}(0). \tag{8}$$

That is, this matrix inner product is the normalized correlation between signals i and j at zero shift (see (3)).

If we could move the elements of one of the matrices around to simulate the process of time shifting the signal, it would be possible to construct values of $\tilde{R}_{ij}(n_\tau T_{\mathrm{c}})$ for other values of n_τ. Specifically, suppose that signal j is shifted by n_τ slot widths relative to signal i so that $a_{n_\tau}^{(i)}$ is multiplied by $a_0^{(j)}$ in the coincidence correlation of (3). The matrix coordinates of $a_{n_\tau}^{(i)}$ are given by the pair β, α of integers which are determined by Euclidean division from n_τ and N_{f} to satisfy the equation

$$n_\tau = \alpha N_{\mathrm{f}} + \beta, \qquad \text{where } 0 \le \beta < N_{\mathrm{f}}. \tag{9}$$

That is, the time shift n_τ corresponds to a shift of α full frame times plus a fraction of a frame time covering β slots. To accomplish the computation

of $\tilde{R}_{ij}(n_\tau T_\mathrm{c})$, the elements of $\mathbf{A}^{(j)}$ must be relocated by a "helical" shift to form the matrix

$$\mathbb{T}_{n_\tau}\mathbf{A}^{(j)} = \begin{bmatrix} a^{(j)}_{\ominus n_\tau} & a^{(j)}_{N_\mathrm{f}\ominus n_\tau} & a^{(j)}_{2N_\mathrm{f}\ominus n_\tau} & \cdots & a^{(j)}_{((N-1)N_\mathrm{f})\ominus n_\tau} \\ a^{(j)}_{1\ominus n_\tau} & a^{(j)}_{(N_\mathrm{f}+1)\ominus n_\tau} & a^{(j)}_{(2N_\mathrm{f}+1)\ominus n_\tau} & \cdots & a^{(j)}_{((N-1)N_\mathrm{f}+1)\ominus n_\tau} \\ \vdots & \vdots & \vdots & \ddots & \vdots \\ a^{(j)}_{(N_\mathrm{f}-1)\ominus n_\tau} & a^{(j)}_{(2N_\mathrm{f}-1)\ominus n_\tau} & a^{(j)}_{(3N_\mathrm{f}-1)\ominus n_\tau} & \cdots & a^{(j)}_{(NN_\mathrm{f}-1)\ominus n_\tau} \end{bmatrix}$$

$$= \left[\begin{array}{cccccc} b^{(j)}_{N_\mathrm{f}-\beta,N-\alpha-1} & \cdots & b^{(j)}_{N_\mathrm{f}-\beta,N-1} & b^{(j)}_{N_\mathrm{f}-\beta,0} & \cdots & b^{(j)}_{N_\mathrm{f}-\beta,N-\alpha-2} \\ \vdots & \ddots & \vdots & \vdots & \ddots & \vdots \\ b^{(j)}_{N_\mathrm{f}-1,N-\alpha-1} & \cdots & b^{(j)}_{N_\mathrm{f}-1,N-1} & b^{(j)}_{N_\mathrm{f}-1,0} & \cdots & b^{(j)}_{N_\mathrm{f}-1,N-\alpha-2} \\ \hline b^{(j)}_{0,N-\alpha} & \cdots & b^{(j)}_{0,0} & b^{(j)}_{0,1} & \cdots & b^{(j)}_{0,N-\alpha-1} \\ \vdots & \ddots & \vdots & \vdots & \ddots & \vdots \\ b^{(j)}_{N_\mathrm{f}-\beta-1,N-\alpha} & \cdots & b^{(j)}_{N_\mathrm{f}-\beta-1,0} & b^{(j)}_{N_\mathrm{f}-\beta-1,1} & \cdots & b^{(j)}_{N_\mathrm{f}-\beta-1,N-\alpha-1} \end{array}\right] \quad (10)$$

Here we have used the operator $\mathbb{T}_{n_\tau}$ to represent the effect of moving the entries of the matrix as indicated in (10).

Because of the way in which this matrix has been constructed, it follows immediately that

$$\left(\mathbf{A}^{(i)}, \mathbb{T}_{n_\tau}\mathbf{A}^{(j)}\right) = \sum_{n=0}^{NN_\mathrm{f}-1} a^{(i)}_n a^{(j)}_{n\ominus n_\tau} = N \cdot \tilde{R}_{ij}(n_\tau T_\mathrm{c}). \quad (11)$$

Notice that all elements in the same row of $\mathbb{T}_{n_\tau}\mathbf{A}^{(j)}$ have the same row index. On the other hand, $b^{(j)}_{mn}$ elements in the same column of $\mathbb{T}_{n_\tau}\mathbf{A}^{(j)}$ have the same column index only if they are on the same side of the line drawn above the row with index 0 in the last matrix in (10). In the special case $\beta = 0$, then all the entries in a column of $\mathbb{T}_{n_\tau}\mathbf{A}^{(j)}$ have the same column index.

2.1 Characterization of a Doubly Periodic Array Design

Typical mathematical array designs that can be found in the literature are constructed to minimize the doubly periodic correlation properties of the arrays. The doubly periodic correlation computation is slightly different than the calculations of the previous section. Let $\mathbf{A}^{(i)}$ and $\mathbf{A}^{(j)}$ be two matrices as defined in (6). The doubly periodic cross-correlation between these two matrices can be defined as

$$P_{\mathbf{A}^{(i)}\mathbf{A}^{(j)}}(n_\mathrm{r}, n_\mathrm{c}) \triangleq \sum_{m=0}^{N_\mathrm{f}-1}\sum_{n=0}^{N-1} b^{(i)}_{m,n} b^{(j)}_{m\ominus n_\mathrm{r}, n\ominus n_\mathrm{c}} \quad (12)$$

for $0 \leq n_{\mathrm{r}} < N_{\mathrm{f}}$ and $0 \leq n_{\mathrm{c}} < N$. Here the computation $\ominus$ is modulo N_{f} in the first subscript and modulo N in the second subscript. To compute this doubly periodic correlation using a matrix inner product, we must transform $\mathbf{A}^{(j)}$ so that its entries are properly positioned to accomplish the computation in (12). This can be done using the $N_{\mathrm{f}} \times N_{\mathrm{f}}$ and $N \times N$ permutation matrices. Let's define an $m \times m$ matrix $\mathbf{P}_m$ to be

$$\mathbf{P}_m \triangleq \begin{bmatrix} 0 & 0 & \dots & 0 & 1 \\ 1 & 0 & \dots & 0 & 0 \\ 0 & 1 & \dots & 0 & 0 \\ \vdots & \vdots & \ddots & \vdots & \vdots \\ 0 & 0 & \dots & 1 & 0 \end{bmatrix} \qquad \text{with} \qquad \mathbf{P}_m^{-1} = \begin{bmatrix} 0 & 1 & 0 & \dots & 0 \\ 0 & 0 & 1 & \dots & 0 \\ \vdots & \vdots & \vdots & \ddots & \vdots \\ 0 & 0 & 0 & \dots & 1 \\ 1 & 0 & 0 & \dots & 0 \end{bmatrix} . \tag{13}$$

Multiplication by $\mathbf{P}_m^n$ on the left of a matrix with m rows cyclically permutes the rows of the matrix n positions downward in the matrix. Similarly, multiplication by $\mathbf{P}_m^{-n}$ on the right of a matrix with m columns cyclically permutes the rows of the matrix n positions to the right in the matrix. Using this notation, it follows immediately that

$$\mathbf{P}_{N_{\mathrm{f}}}^{n_{\mathrm{r}}} \, \mathbf{A}^{(j)} \, \mathbf{P}_N^{-n_{\mathrm{c}}} = \tag{14}$$

$$\left[\begin{array}{ccccc|ccccc} b^{(j)}_{N_{\mathrm{f}}-n_{\mathrm{r}},N-n_{\mathrm{c}}} & \dots & b^{(j)}_{N_{\mathrm{f}}-n_{\mathrm{r}},0} & b^{(j)}_{N_{\mathrm{f}}-n_{\mathrm{r}},1} & \dots & b^{(j)}_{N_{\mathrm{f}}-n_{\mathrm{r}},N-n_{\mathrm{c}}-1} \\ \vdots & \ddots & \vdots & \vdots & \ddots & \vdots \\ b^{(j)}_{N_{\mathrm{f}}-1,N-n_{\mathrm{c}}} & \dots & b^{(j)}_{N_{\mathrm{f}}-1,0} & b^{(j)}_{N_{\mathrm{f}}-1,1} & \dots & b^{(j)}_{N_{\mathrm{f}}-1,N-n_{\mathrm{c}}-1} \\ \hline b^{(j)}_{0,N-n_{\mathrm{c}}} & \dots & b^{(j)}_{0,0} & b^{(j)}_{0,1} & \dots & b^{(j)}_{0,N-n_{\mathrm{c}}-1} \\ \vdots & \ddots & \vdots & \vdots & \ddots & \vdots \\ b^{(j)}_{N_{\mathrm{f}}-n_{\mathrm{r}}-1,N-n_{\mathrm{c}}} & \dots & b^{(j)}_{N_{\mathrm{f}}-n_{\mathrm{r}}-1,0} & b^{(j)}_{N_{\mathrm{f}}-n_{\mathrm{r}}-1,1} & \dots & b^{(j)}_{N_{\mathrm{f}}-n_{\mathrm{r}}-1,N-n_{\mathrm{c}}-1} \end{array}\right]$$

and it follows that

$$\left(\mathbf{A}^{(i)}, \mathbf{P}_{N_{\mathrm{f}}}^{n_{\mathrm{r}}} \mathbf{A}^{(j)} \mathbf{P}_N^{-n_{\mathrm{c}}}\right) = P_{\mathbf{A}^{(i)}\mathbf{A}^{(j)}}(n_{\mathrm{r}}, n_{\mathrm{c}}) . \tag{15}$$

2.2 Relation between Time-Hopping and a Doubly Periodic Array Design

A comparison of (10) and (15) indicates that the bottom $N_{\mathrm{f}} - \beta$ rows of $\mathbb{T}_{n_\tau}\mathbf{A}^{(j)}$ are identical to the bottom $N_{\mathrm{f}} - \beta$ rows $\mathbf{P}_{N_{\mathrm{f}}}^{\beta}\mathbf{A}^{(j)}\mathbf{P}_N^{-\alpha}$. We can write this mathematically as

$$\mathbf{L}_{N_{\mathrm{f}}-\beta \times N_{\mathrm{f}}}\left[\mathbb{T}_{n_\tau}\mathbf{A}^{(j)}\right] = \mathbf{L}_{N_{\mathrm{f}}-\beta \times N_{\mathrm{f}}}\mathbf{P}_{N_{\mathrm{f}}}^{\beta}\mathbf{A}^{(j)}\mathbf{P}_N^{-\alpha} \tag{16}$$

where generally

$$\mathbf{L}_{N_1 \times N_2} = [\mathbf{O}_{N_1 \times N_2 - N_1} \quad \mathbf{I}_{N_1}] \tag{17}$$

operates on the left of a matrix with N_2 rows to reduce the matrix to its last N_1 rows. Of course, generally $\mathbf{I}_N$ denotes an $N \times N$ identity matrix and $\mathbf{O}_{N_1 \times N_2}$ denotes an all-zeros matrix of the indicated dimension. A similar comparison of the upper β rows of $\mathbb{T}_{n_\tau}\mathbf{A}^{(j)}$ and $\mathbf{P}_{N_\mathrm{f}}^{\beta}\mathbf{A}^{(j)}\mathbf{P}_N^{-(\alpha+1)}$ in (10) and (15) respectively yields

$$\mathbf{U}_{\beta \times N_\mathrm{f}}\left[\mathbb{T}_{n_\tau}\mathbf{A}^{(j)}\right] = \mathbf{U}_{\beta \times N_\mathrm{f}}\mathbf{P}_{N_\mathrm{f}}^{\beta}\mathbf{A}^{(j)}\mathbf{P}_N^{-(\alpha+1)}\,, \tag{18}$$

where generally

$$\mathbf{U}_{N_1 \times N_2} = [\mathbf{I}_{N_1} \quad \mathbf{O}_{N_2 - N_1}] \tag{19}$$

selects the upper N_1 rows on which it operates. Together (16) and (18) create a representation for $\mathbb{T}_{n_\tau}\mathbf{A}^{(j)}$ in terms of doubly cyclic shifts of $\mathbf{A}^{(j)}$, namely

$$\mathbb{T}_{n_\tau}\mathbf{A}^{(j)} = \begin{bmatrix} \mathbf{U}_{\beta \times N_\mathrm{f}}\mathbf{P}_{N_\mathrm{f}}^{\beta}\mathbf{A}^{(j)}\mathbf{P}_N^{-(\alpha+1)} \\ \mathbf{L}_{N_\mathrm{f}-\beta \times N_\mathrm{f}}\mathbf{P}_{N_\mathrm{f}}^{\beta}\mathbf{A}^{(j)}\mathbf{P}_N^{-\alpha} \end{bmatrix} \tag{20}$$

Substituting the above representation into (11) and simplifying with (15) gives

$$\begin{aligned}
\tilde{R}_{ij}(n_\tau T_\mathrm{c}) &= \frac{1}{N}\left(\mathbf{A}^{(i)}, \begin{bmatrix} \mathbf{U}_{\beta \times N_\mathrm{f}}\mathbf{P}_{N_\mathrm{f}}^{\beta}\mathbf{A}^{(j)}\mathbf{P}_N^{-(\alpha+1)} \\ \mathbf{L}_{N_\mathrm{f}-\beta \times N_\mathrm{f}}\mathbf{P}_{N_\mathrm{f}}^{\beta}\mathbf{A}^{(j)}\mathbf{P}_N^{-\alpha} \end{bmatrix}\right) \\
&= \frac{1}{N}\left(\begin{bmatrix} \mathbf{U}_{\beta \times N_\mathrm{f}}\mathbf{A}^{(i)} \\ \mathbf{L}_{N_\mathrm{f}-\beta \times N_\mathrm{f}} \quad \mathbf{A}^{(i)} \end{bmatrix}, \begin{bmatrix} \mathbf{U}_{\beta \times N_\mathrm{f}}\mathbf{P}_{N_\mathrm{f}}^{\beta}\mathbf{A}^{(j)}\mathbf{P}_N^{-(\alpha+1)} \\ \mathbf{L}_{N_\mathrm{f}-\beta \times N_\mathrm{f}}\mathbf{P}_{N_\mathrm{f}}^{\beta}\mathbf{A}^{(j)}\mathbf{P}_N^{-\alpha} \end{bmatrix}\right) \\
&= \frac{1}{N}\left(\mathbf{U}_{\beta \times N_\mathrm{f}}\mathbf{A}^{(i)}, \mathbf{U}_{\beta \times N_\mathrm{f}}\mathbf{P}_{N_\mathrm{f}}^{\beta}\mathbf{A}^{(j)}\mathbf{P}_N^{-(\alpha+1)}\right) \\
&\quad + \frac{1}{N}\left(\mathbf{L}_{N_\mathrm{f}-\beta \times N_\mathrm{f}}\mathbf{A}^{(i)}, \mathbf{L}_{N_\mathrm{f}-\beta \times N_\mathrm{f}}\mathbf{P}_{N_\mathrm{f}}^{\beta}\mathbf{A}^{(j)}\mathbf{P}_N^{-\alpha}\right) \\
&\leq \frac{1}{N}\left(\mathbf{A}^{(i)}, \mathbf{P}_{N_\mathrm{f}}^{\beta}\mathbf{A}^{(j)}\mathbf{P}_N^{-(\alpha+1)}\right) + \frac{1}{N}\left(\mathbf{A}^{(i)}, \mathbf{P}_{N_\mathrm{f}}^{\beta}\mathbf{A}^{(j)}\mathbf{P}_N^{-\alpha}\right) \\
&= \frac{1}{N}\left[P_{\mathbf{A}^{(i)}\,\mathbf{A}^{(j)}}(\beta, \alpha+1) + P_{\mathbf{A}^{(i)}\,\mathbf{A}^{(j)}}(\beta, \alpha)\right]\,.
\end{aligned} \tag{21}$$

where α and β are determined by (9). The inequality comes from the fact that all entries in these matrices are non-negative, and multiplication by the row selectors $\mathbf{U}_{\beta \times N_\mathrm{f}}$ and $\mathbf{L}_{N_\mathrm{f}-\beta \times N_\mathrm{f}}$ simply reduces the range of the row index in the inner product computation.

Notice that (21) is a bound on time hopping correlation values in terms of a sum of two doubly periodic correlation values.

Hence, a set of M matrices $\mathbf{A}^{(i)}$, $i = 1, \ldots, M$, with non-matched doubly periodic correlation at most

$$P_{max}\left(\{\mathbf{A}^{(i)}\}_{i=1}^{M}\right) \triangleq \max_{\substack{i,\,j,\,n_\mathrm{r},\,n_\mathrm{c}: \\ i \neq j \text{ or } n_\mathrm{r} \neq 0 \text{ or } n_\mathrm{c} \neq 0}} P_{\mathbf{A}^{(i)}\,\mathbf{A}^{(j)}}(n_\mathrm{r}, n_\mathrm{c})\,, \tag{22}$$

can be mapped into a set of M time-hopping sequences (using (4)) with the normalized correlation bound

$$\max_{\substack{i,\,j,\,n_\tau: \\ i \neq j \text{ or } n_\tau \neq 0}} \tilde{R}_{ij}(n_\tau T_c) \leq \frac{2}{N} P_{\max}\left(\{\mathbf{A}^{(i)}\}_{i=1}^{M}\right). \tag{23}$$

When necessary, it is not difficult to adapt this correlation bounding approach to include guard times between pulse frames and other implementation constraints, by inserting mandatory rows of zeros in the $\mathbf{A}^{(i)}$ matrices.

2.3 The Johnson Bound

The Johnson bound (see [3] page 327, and [4]) is a bound on the number of constant-weight words that can be achieved in the design of a cyclic code with a prescribed minimum Hamming distance. Viewing our sequences $\{a_n^{(i)}\}_{i=1}^{M}$ and their cyclic shifts as constant weight cyclic code words over the binary field of two elements, we can transform the Johnson bound to one on the number of time-hopping sequences that can be designed with a prescribed upper bound on auto- and cross-correlation.

Clearly, the design objective is to minimize the periodic correlations $N\tilde{R}_{i,j}(n_\tau T_w)$ except when $i = j$ and $n_\tau = 0$ in which case $N\tilde{R}_{i,j}(n_\tau T_w) = N$. Let there be M time-hopping sequences in all. If we impose the condition

$$N\tilde{R}_{i,j}(n_\tau T_w) \;\leq\; \lambda, \text{ when either } i \neq j \text{ or } n_\tau \neq 0, \tag{24}$$

by specification of the parameter λ, then the Johnson bound states that

$$M \leq \left\lfloor \frac{1}{N} \left\lfloor \frac{NN_f - 1}{N-1} \cdots \left\lfloor \frac{NN_f - (\lambda-1)}{N-(\lambda-1)} \left\lfloor \frac{NN_f - \lambda}{N-\lambda} \right\rfloor \right\rfloor \cdots \right\rfloor \right\rfloor \tag{25}$$

where N is the weight of the sequence, NN_f is the sequence period, and $\lfloor a \rfloor$ denotes the largest integer $\leq a$. When both N and N_f are large and λ is small, the bound can be approximated by

$$M \leq \frac{(NN_f)^\lambda}{N^{\lambda+1}} \;=\; \frac{N_f^\lambda}{N}. \tag{26}$$

Note that unless $N_f >> N$, setting $\lambda = 1$ would result in a small number of time-hopping sequences. Thus the Johnson bound indicates that $\lambda = 2$ is the smallest value for which a multiple-access signal design may be feasible.

2.4 A Time-Hopping Construction with $\lambda = 2$

Let GF(p) denote the finite field with arithmetic modulo a prime p. Let $\mathcal{F}$ denote the set of all polynomials of degree at most 2 with coefficients in GF(p). That is, the i-th polynomial in $\mathcal{F}$ is of the form

$$f^{(i)}(x) = f_2^{(i)} x^2 \oplus f_1^{(i)} x \oplus f_0^{(i)}, \qquad f_2^{(i)}, f_1^{(i)}, f_0^{(i)} \in \mathrm{GF}(p), \tag{27}$$

where $\oplus$ denotes addition modulo p. To each polynomial $f^{(i)}(x)$ in $\mathcal{F}$ we associate a $p \times p$ matrix $\tilde{\mathbf{A}}^{(i)} = [\tilde{b}^{(i)}_{m,n}]$ with elements defined by

$$\tilde{b}^{(i)}_{m,n} = \begin{cases} 1 & \text{if } f^{(i)}(n) = m, \quad 0 \le m \le p-1,\ 0 \le n \le p-1 \\ 0 & \text{otherwise.} \end{cases} \tag{28}$$

That is, the row location m of the 1 in column n in $\tilde{\mathbf{A}}^{(i)}$ is given by $f^{(i)}(n)$. As a result, the matrix $\tilde{\mathbf{A}}^{(i)}$ will have a single 1 in each column.

Let $\tilde{\mathbf{A}}^{(i)}$ and $\tilde{\mathbf{A}}^{(j)}$ denote two matrices corresponding to polynomials $f^{(i)}(x)$ and $f^{(j)}(x)$ belonging to $\mathcal{F}$. Following the development of (15), the doubly periodic correlation $P_{\tilde{\mathbf{A}}^{(i)}\tilde{\mathbf{A}}^{(j)}}(n_\mathrm{r}, n_\mathrm{c})$ of the matrices $\tilde{\mathbf{A}}^{(i)}$ and $\tilde{\mathbf{A}}^{(j)}$ is given by

$$\begin{aligned} P_{\tilde{\mathbf{A}}^{(i)}\tilde{\mathbf{A}}^{(j)}}(n_\mathrm{r}, n_\mathrm{c}) &= \left(\tilde{\mathbf{A}}^{(i)}, \mathbf{P}^{n_\mathrm{r}}_{N_\mathrm{a}} \tilde{\mathbf{A}}^{(j)} \mathbf{P}^{-n_\mathrm{c}}_{N}\right) \\ &= \left|\left\{x:\ f^{(i)}(x) = f^{(j)}(x \ominus n_\mathrm{c}) \oplus n_\mathrm{r},\ 0 \le x \le p-1\right\}\right| \end{aligned} \tag{29}$$

The last equality above comes from counting the number of column indices x in which $\tilde{\mathbf{A}}^{(i)}$ and $\mathbf{P}^{n_\mathrm{r}}_{N_\mathrm{a}} \tilde{\mathbf{A}}^{(j)} \mathbf{P}^{-n_\mathrm{c}}_{N}$ have identical row locations for their 1's. Each such correspondence contributes a 1 to the correlation value. Since $f^{(i)}(x)$ and $f^{(j)}(x)$ are both of degree 2 over a field, the row matching equation on the right in (29) can have at most two solutions except when the polynomials on the two sides of the equation above are identical. We now insure that the latter situation can happen only when $i = j$ and $n_\mathrm{c} = n_\mathrm{r} = 0$.

The condition for row matching can be reduced as follows:

$$\begin{aligned} & f^{(i)}(x) = f^{(j)}(x \ominus n_\mathrm{c}) \oplus n_\mathrm{r} \\ \iff & f^{(i)}_2 x^2 \oplus f^{(i)}_1 x \oplus f^{(i)}_0 = f^{(j)}_2 (x \ominus n_\mathrm{c})^2 \oplus f^{(j)}_1 (x \ominus n_\mathrm{c}) \oplus f^{(j)}_0 \oplus n_\mathrm{r} \\ \iff & \begin{cases} \left(f^{(i)}_2 \ominus f^{(j)}_2\right) x^2 \oplus \left(f^{(i)}_1 \oplus 2 f^{(j)}_2 n_\mathrm{c} \ominus f^{(j)}_1\right) x \\ \qquad \oplus \left(f^{(i)}_0 \ominus f^{(j)}_2 n_\mathrm{c}^2 \oplus f^{(j)}_1 n_\mathrm{c} \ominus f^{(j)}_0 \ominus n_\mathrm{r}\right) = 0 \quad \text{for } i \ne j \\ \left(2 f^{(j)}_2 n_\mathrm{c}\right) x \oplus \left(\ominus f^{(j)}_2 n_\mathrm{c}^2 \oplus f^{(j)}_1 n_\mathrm{c} \ominus n_\mathrm{r}\right) = 0 \quad \text{for } i = j\,. \end{cases} \end{aligned} \tag{30}$$

The polynomial for the case $i \ne j$ above will never disappear and will always have degree 2 if we require that $f^{(i)}_2 \ne f^{(j)}_2$ for all $i \ne j$. In addition, the polynomial for the case for $i = j$ in (30) will not disappear if $f^{(j)}_2 \ne 0$ for all j unless $n_\mathrm{c} = n_\mathrm{r} = 0$ (the no-shift condition for peak auto-correlation N). Hence we have arrived at the following result.

Let p be any prime number. The set of $p-1$ polynomials

$$f^{(i)}(x) = ix^2 \quad \textit{for } i = 1, 2, \ldots, p-1, \tag{31}$$

can be used to construct (using (28) and (31)) a set of $p \times p$ binary signal matrices $\{\tilde{\mathbf{A}}^{(i)}\}_{i=1}^{M}$ with unmatched doubly periodic auto-correlation at most 1 and cross-correlation at most 2.

As an Example, with $p = 11$ we can construct the sequence design illustrated in Table 1.

$i \setminus j$	0	1	2	3	4	5	6	7	8	9	10
1	0	1	4	9	5	3	3	5	9	4	1
2	0	2	8	7	10	6	6	10	7	8	2
3	0	3	1	5	4	9	9	4	5	1	3
4	0	4	5	3	9	1	1	9	3	5	4
5	0	5	9	1	3	4	4	3	1	9	5
6	0	6	2	10	8	7	7	8	10	2	6
7	0	7	6	8	2	10	10	2	8	6	7
8	0	8	10	6	7	2	2	7	6	10	8
9	0	9	3	4	1	5	5	1	4	3	9
10	0	10	7	2	6	8	8	6	2	7	10

$$\mathbf{A}^{(3)} = \begin{bmatrix} 1 & 0 & 0 & 0 & 0 & 0 & 0 & 0 & 0 & 0 & 0 \\ 0 & 0 & 1 & 0 & 0 & 0 & 0 & 0 & 0 & 1 & 0 \\ 0 & 0 & 0 & 0 & 0 & 0 & 0 & 0 & 0 & 0 & 0 \\ 0 & 1 & 0 & 0 & 0 & 0 & 0 & 0 & 0 & 0 & 1 \\ 0 & 0 & 0 & 0 & 1 & 0 & 0 & 1 & 0 & 0 & 0 \\ 0 & 0 & 0 & 1 & 0 & 0 & 0 & 0 & 1 & 0 & 0 \\ 0 & 0 & 0 & 0 & 0 & 0 & 0 & 0 & 0 & 0 & 0 \\ 0 & 0 & 0 & 0 & 0 & 0 & 0 & 0 & 0 & 0 & 0 \\ 0 & 0 & 0 & 0 & 0 & 0 & 0 & 0 & 0 & 0 & 0 \\ 0 & 0 & 0 & 0 & 0 & 1 & 1 & 0 & 0 & 0 & 0 \\ 0 & 0 & 0 & 0 & 0 & 0 & 0 & 0 & 0 & 0 & 0 \end{bmatrix}$$

Table 1. Complete family for $p = 11$ in $c_j^{(i)}$ form and matrix for $i = 3$

The Johnson Bound states that for a collection of $p \times p$ matrices with $\lambda = 2$ corresponding to a time-hopping design with $p = N_\mathrm{f} = N$ and p large, there can be at most $p + 3$ matrices in the collection. Hence this design is within 4 matrices of being tight with respect to the Johnson bound.

The proposed set of time-hopping patterns associated with the matrices $\{\tilde{\mathbf{A}}^{(i)}\}_{i=1}^{M}$ in this design can have a non-matched normalized correlation of at most $2\lambda/N = 4/N$ (see (21)). Hence for example, a value of $p = 4093$ will provide 4092 distinct time-hopping patterns $a_n^{(i)}$ of period equal to $4093N_\mathrm{f}$ with no two patterns having coincidences in more than four pulse positions over the sequence period, regardless of the relative time shift between patterns. Other time-hopping designs were presented in [5], and more can be adapted from the frequency-hopping sequence literature [6].

3 Power Spectral Density Computations

The ability to design a UWB signal set with a flat power spectral density (PSD) is one key to successful UWB signal design. In principle, the flatter the power spectral density of the transmission, the larger the amount of power that can be radiated while still satisfying PSD bounds imposed by regulatory agencies. Such tests may be done on the UWB carrier without data modulation.

A wide variety of UWB carriers can be modeled in the simple form

$$s^{(i)}(t) = \sum_n a_n^{(i)} p(t - nT_\mathrm{c}) \,, \tag{32}$$

where the $\{a_n^{(i)}\}$ are real numbers. This model embraces both time-hopping ($a_n^{(i)} \in \{0, 1\}$) and direct-sequence ($a_n^{(i)} \in \{1, -1\}$) spread-spectrum signals.

Here, we assume that the period of the sequences $\{a_n^{(i)}\}$ is N, and use i to represent the user index. One way of mathematically modeling the generation of these signals is shown in Figure 2. The impulse response $h_{\rm op}^{(i)}(t)$ of the one-period sequence generator for the $i^{\rm th}$ waveform is

$$h_{\rm op}^{(i)}(t) = \sum_{n=0}^{N-1} a_n^{(i)} \delta(t - nT_{\rm c}) \tag{33}$$

where $\delta(t)$ is the Dirac delta function. The impulse response of the pulse shaping circuit is simply $p(t)$.

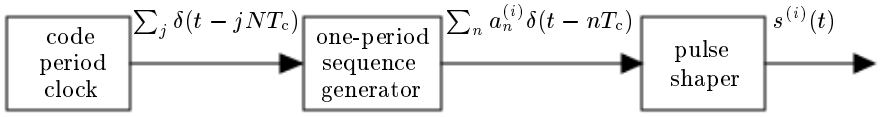

Fig. 2. Mathematical model of a UWB signal generator without data modulation.

Because the output of the code period clock has period $NT_{\rm c}$, it is easily verified that the output has PSD $S_{\rm cpc}(f)$ given by a sum of Dirac delta functions of equal area at multiples of $(NT_{\rm c})^{-1}$,

$$S_{\rm cpc}(f) = \frac{1}{(NT_{\rm c})^2} \sum_k \delta\left(f - \frac{k}{NT_{\rm c}}\right) . \tag{34}$$

The system function of the one-step sequence generator is

$$H_{\rm op}^{(i)}(f) = \mathbb{F}\left\{h_{\rm op}^{(i)}(t)\right\} = \sum_{n=0}^{N-1} a_n^{(i)} e^{-j2\pi f n T_{\rm c}} , \tag{35}$$

where $\mathbb{F}\{\cdot\}$ denotes the Fourier transform operation. The system function of the pulse shaper is simply the Fourier transform $P(f)$ of the pulse shape $p(t)$. It follows immediately that the PSD of the signal $s^{(i)}(t)$ is

$$\begin{aligned} S_{s^{(i)}}(f) &= \left|P(f)H_{\rm op}^{(i)}(f)\right|^2 S_{\rm cpc}(f) \\ &= |P(f)|^2 \left|\sum_{n=0}^{N-1} a_n^{(i)} e^{-j2\pi f n T_{\rm c}}\right|^2 \frac{1}{(NT_{\rm c})^2} \sum_k \delta\left(f - \frac{k}{NT_{\rm c}}\right) \\ &= \frac{|P(f)|^2}{(NT_{\rm c})^2} \sum_k C_k^{(i)} \delta\left(f - \frac{k}{NT_{\rm c}}\right) , \end{aligned} \tag{36}$$

where

$$C_k^{(i)} = \left|\sum_{n=0}^{N-1} a_n^{(i)} e^{-j2\pi k n/N}\right|^2 . \tag{37}$$

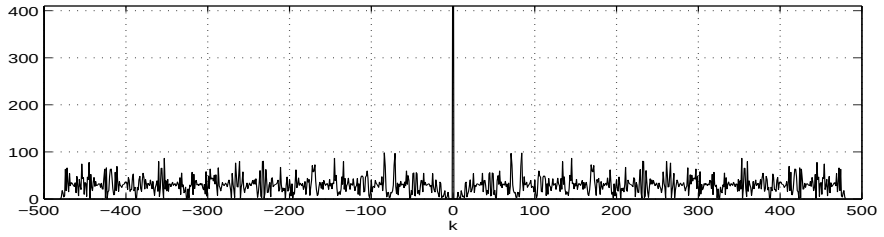

Fig. 3. C_k^{15} of quadratic construction (eq. 31) with p=31 (peak value 961 at k=0).

Hence, the coefficients $\{C_k^{(i)}\}$ represent the effect of code design on the PSD of the UWB signal $s^{(i)}(t)$ without data modulation. The coefficients are periodic, i.e., $C_k^{(i)} = C_{k+N}^{(i)}$, and because the $\{a_n^{(i)}\}$ are real, also possess a symmetry, namely $C_k^{(i)} = C_{-k}^{(i)}$ for all k and i. In Figure 3 we show the C_k^{15} of a signal using the quadratic sequence construction with $p = 31$.

3.1 Spectral Flatness

The emphasis for many years has been on sequence design for low auto- and cross-correlation. However, repeated structures in the sidelobes of the autocorrelation of a sequence, even if small, can cause lines of uneven height in the spectral density of the sequence.

To make the PSD of (36) as flat as possible (see [5]), one could try to design the coefficients of (37) so that $C_k^{(i)}$ are inversely proportional to $|P(\frac{k}{NT_c})|^2$. This is a difficult problem because of (a) the constraints that are caused by the allowable choices for $a_n^{(i)}$ and (b) the symmetries and periodicities of the $\{C_k^{(i)}\}$ sequence. The alternative design objective that we shall use here, which is independent of the choice of pulse shape, is to make the values of $C_k^{(i)}$, $k = 0, 1, \ldots, \lceil N/2 \rceil - 1$, as uniformly small as possible, the remainder of the values of $C_k^{(i)}$ for other k then being determined by periodicity and symmetry.

Expanding (37) gives some insight into designing for spectral flatness in pure time-hopping signals ($a_m^{(i)} \in \{0, 1\}$). Then

$$C_k^{(i)} = \sum_{m=0}^{N-1} \sum_{n=0}^{N-1} a_m^{(i)} a_n^{(i)} e^{j2\pi k(m-n)/N} = \sum_{r=0}^{N-1} N_r e^{j2\pi kr/N} \tag{38}$$

where N_r is the number of times that the product $a_m^{(i)} a_n^{(i)} = 1$ when $m - n = r \mod N$ as m and n range from 0 to $N - 1$, i.e.,

$$N_r = \left|\left\{m : a_m^{(i)} = a_{m+r \mod N}^{(i)} = 1, \quad 0 \le m < N\right\}\right|. \tag{39}$$

The number of pulses in one period of the sequence is N_0, and $C_0^{(i)} = N_0^2$ regardless of the location of the pulses within a period of the sequence. The spectral coefficients can be summed over k to give

$$\sum_{k=0}^{N-1} C_k^{(i)} = \sum_{m=0}^{N-1} \sum_{n=0}^{N-1} a_m^{(i)} a_n^{(i)} \sum_{k=0}^{N-1} e^{j2\pi k(m-n)/N} = NN_0\,, \tag{40}$$

and therefore the average value of the spectral coefficients for $k \neq 0$ is

$$C_{\text{avg}} \triangleq \frac{1}{N-1} \sum_{k=1}^{N-1} C_k^{(i)} = \frac{NN_0 - N_0^2}{N-1} \tag{41}$$

If the spectral coefficients are to be identical for $k \neq 0 \mod N$, then it must follow that $C_k^{(i)} = C_{\text{avg}}$ for these k. This is an ideal sequence design goal.

Now suppose that each value of N_r, $r \neq 0 \mod N$, is identical, i.e.,

$$N_r = N_{\text{avg}} \triangleq (N-1)^{-1} \sum_{r=1}^{N-1} N_r = \frac{N_0^2 - N_0}{N-1} \quad \forall\, r \neq 0 \mod N\,. \tag{42}$$

Then it follows immediately from (38) that

$$C_k^{(i)} = \begin{cases} N_0^2 & \text{if } k = 0 \mod N \\ N_0 - N_{\text{avg}} = C_{\text{avg}} & \text{otherwise.} \end{cases} \tag{43}$$

The condition (42) is that of a difference set design with the values of n for which $a_n^{(i)} = 1$ forming a (N, N_0, N_{avg}) cyclic difference set [7],[8].

3.2 Multiple Access Designs for Spectral Flatness

Certainly individual sequence designs with the ideal spectral coefficients of (43) are possible. However the collection of difference sets for any choice of the parameter set (N, N_0, N_{avg}) appears to be small, and there is no guarantee that the sequence designs corresponding to these sets have the good cross-correlation properties that are desirable for asynchronous multiple access communications.

One design [9] that meets the Welch bound on cross-correlation and hence has good multiple access capabilities is constructed using a difference set and a Hadamard matrix. Specifically, each sequence is constructed using the same difference set to specify the location of the non-zero elements of the sequence. Hence, when the sequences are not time synchronized, the difference set property guarantees low cross-correlation because of a low number of coincidences. To guarantee zero cross-correlation when two such sequences have their non-zero elements in complete synchronism, each sequence in the set uses as its non-zero elements a different row of an $N_0 \times N_0$ Hadamard matrix. With

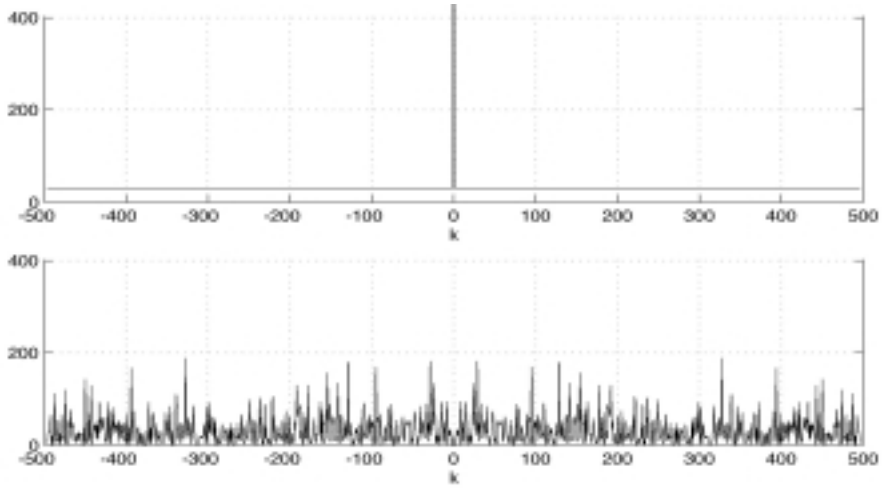

Fig. 4. Spectral coefficients $C_k^{(i)}$ of difference set (993,32,1) with the all ones vector with peak value at 1024 (top) and with a typical Hadamard vector (bottom).

the Hadamard matrix constructed to have a row filled completely with +1s, there is at least one sequence in the collection with spectral coefficients satisfying (43). A plot of the spectral coefficients for two sequences from a design based on a (993,32,1) cyclic difference set and a 32×32 Hadamard matrix are shown in Figure 4. Certainly there are sequences in this design that do not have spectral coefficients satisfying the spectral flatness condition (43).

4 Closing Thoughts: More Problems

There are challenging problems buried in the details of UWB signal design. An example of a design problem that is exacerbated in UWB systems is the acquisition of sequence synchronization. If we assume that the time and/or complexity required to achieve synchronization is proportional to the number of correlations that the receiver has to compute in the sync search process, then a full search over a timing uncertainty interval of T_{unc} will have acquisition-time$\times$complexity proportional to $T_{\text{unc}}/T_{\text{res}}$, the quantity T_{res} being the time resolution capability of the UWB signal. For example, a one nanosecond time-resolution used in a system with an initial timing uncertainty equivalent to a spreading code period of one millisecond means that the receiver must compute 10^6 correlations. This acquisition problem is easily a few orders of magnitude more difficult than that for narrowband systems with the same initial uncertainty T_{unc}.

Embedding simple aids to acquisition can be done in many ways, from putting a known header in front of the sequence, to simultaneously transmitting an easily acquired signal of known relative timing to the UWB signal.

One of the more interesting approaches, proposed by Stiffler [10] for a single signal design, used $\log_2(T_{\rm unc}/T_{\rm res})$ correlations to resolve the timing uncertainty of the signal. The challenging **problem** to the sequence designer is to build sets of sequences that not only have good correlation properties and flat spectra, but which also are amenable to rapid acquisition techniques. Generally rapid acquisition wil cost something in the design process, possibly some non-flatness in the power spectral density, an increase in the operating signal-to-noise ratio, etc.

Another **problem** is to design sequences to have lowered power-spectral densities in certain portions of the frequency domain. While spectral flatness is in principle desirable, anticipated regulations may require lowered UWB power densities in certain portions of the frequency domain. Can this be achieved partially or fully in some organized way by sequence design?

5 Acknowledgement

The authors wish to thank the Time Domain Corporation for its continued interest and support of this research. Portions of this work have been reprinted with permission of the Time Domain Corporation.

References

1. R. A. Scholtz et al., "Ultra-wideband Radio Deployment Challenges," *PIMRC 2000*, London, UK, Session 5, Paper 1 (invited), September 18-21, 2000.
2. R. A. Scholtz, "Multiple-Access with Time-Hopping Impulse Modulation," *MILCOM '93,* Boston, MA, October 11-14, 1993.
3. F. J. MacWilliams and N. J. A. Sloane, *The Theory of Error Correcting Codes*, North-Holland, New York, 1983.
4. O. Moreno, Z. Zhang, P. V. Kumar and V. Zinoviev, "New Constructions of Optimal Cyclically Permutable Constant Weight Code," *IEEE Trans. Inform. Theory*, vol. 41, pp.448-456, March 1995.
5. C. J. Corrada-Bravo, R. A. Scholtz, and P. V. Kumar "Generating TH-SSMA sequences with good correlation and low PSD level," *1999 UWB Conference for Radio and Radar Technology,* Washington DC, Sept. 26-28, 1999.
6. M. Simon, J. Omura, R. Scholtz, B. Levitt, *Spread Spectrum Communications Handbook*, McGraw-Hill, 1994.
7. L. Baumert, *Cyclic Difference Sets*, Lecture Notes in Mathematics, vol. 182, Springer-Verlag, 1971.
8. A. Pott, P.V. Kumar, T. Helleseth, D. Jungnickel, Difference Sets, Sequences and Their Correlation Properties. Holland, September 1999.
9. R. A. Scholtz, "Optimum CDMA Codes," *Proc. of the National Telecommunications Conference*, November 1979.
10. J. J. Stiffler, "Rapid Acquisition Sequences," *IEEE Trans. Inform. Theory*, IT-14, p. 221-225, 1968.